CAIT-UTC-REG71

# Bio-Mediated Method for Improving the Erosion Resistance of Coastal Embankments

FINAL REPORT
December 2024

Submitted by:

Cheng Zhu, Ph.D., P.E.
Associate Professor
Department of Civil and Environmental Engineering
Rowan University
201 Mullica Hill Road
Glassboro, NJ, 08028

Kaniz Roksana
Graduate Research Fellow
Department of Civil and Environmental Engineering
Rowan University
201 Mullica Hill Road
Glassboro, NJ, 08028

External Project Manager

Theresa Loux, Ph.D., P.E.
Chief Technical Officer
Aero Aggregates of North America

In cooperation with

Rutgers, The State University of New Jersey
And
State of New Jersey
Department of Transportation
And
U.S. Department of Transportation
Federal Highway Administration

**Disclaimer Statement**

The contents of this report reflect the views of the authors, who are responsible for the facts and the accuracy of the information presented herein. This document is disseminated under the sponsorship of the Department of Transportation, University Transportation Centers Program, in the interest of information exchange. The U.S. Government assumes no liability for the contents or use thereof.

The Center for Advanced Infrastructure and Transportation (CAIT) is a Regional UTC Consortium led by Rutgers, The State University. Members of the consortium are Atlantic Cape Community College, Columbia University, Cornell University, New Jersey Institute of Technology, Polytechnic University of Puerto Rico, Princeton University, Rowan University, SUNY - Farmingdale State College, and SUNY - University at Buffalo. The Center is funded by the U.S. Department of Transportation.

| | | | |
|---|---|---|---|
| 1. Report No.<br>CAIT-UTC-REG71 | 2. Government Accession No. | 3. Recipient's Catalog No. | |
| 4. Title and Subtitle<br>Bio-Mediated Method for Improving the Erosion Resistance of Coastal Embankments | | 5. Report Date<br>December 2024 | |
| | | 6. Performing Organization Code<br>CAIT/Rowan University | |
| 7. Author(s)<br>Cheng Zhu (0000-0001-5382-1003)<br>Kaniz Roksana (0000-0002-8088-9043) | | 8. Performing Organization Report No.<br>CAIT-UTC-REG71 | |
| 9. Performing Organization Name and Address<br>Department of Civil and Environmental Engineering<br>Rowan University<br>201 Mullica Hill Road, Glassboro, NJ, 08028 | | 10. Work Unit No. | |
| | | 11. Contract or Grant No.<br>69A3551847102 | |
| 12. Sponsoring Agency Name and Address<br>Center for Advanced Infrastructure and Transportation<br>Rutgers, The State University of New Jersey<br>100 Brett Road<br>Piscataway, NJ 08854 | | 13. Type of Report and Period Covered<br>Final Report<br>7/1/2022 – 3/312025 | |
| | | 14. Sponsoring Agency Code | |
| 15. Supplementary Notes<br>U.S. Department of Transportation/OST-R<br>1200 New Jersey Avenue, SE<br>Washington, DC 20590-0001 | | | |
| 16. Abstract<br>Due to extreme weather events, coastal embankments are subjected to more frequent storm wave inundation and surge impacts, contributing to widespread coastal erosion problems. This research explored an innovative bio-mediated approach utilizing enzymatic-induced carbonate precipitation (EICP) to assess its efficacy in addressing issues related to coastal erosion. To comprehensively evaluate the outcomes of bio-cementation and its effectiveness in stabilizing coastal slopes, it is crucial to first quantify and compare various properties of EICP-treated soils, including hydraulic conductivity and strength parameters. Small-scale laboratory erosion tests were also conducted on both EICP-treated and untreated sandy slopes, with continuous monitoring of the cross-shore profile. Erosion volumes above the still water level and slope reductions beneath the water surface were calculated based on the recorded bed profiles. The findings indicate a significant reduction in sandy slope erosion under wave conditions with the application of EICP. Microstructure analysis further reveals that EICP treatment results in interlocking cementation among sand particles, substantially enhancing the sand's resistance to erosion. This research developed a bio-mediated technique to improve the physical properties of local coastal sand and showed its great potential for coastal erosion mitigation in New Jersey. | | | |
| 17. Key Words<br>embankment stability, bio-mediated technology, ground improvement, coastal erosion | | 18. Distribution Statement | |
| 19. Security Classification (of this report)<br>Unclassified | 20. Security Classification (of this page)<br>Unclassified | 21. No. of Pages<br>29 | 22. Price |

**Form DOT F 1700.7** (8-69)

## Table of Contents

## List of Figures

## List of Tables

## 1 Introduction

Developed coastal areas frequently encounter erosion hazards, resulting in damage to property and loss of human life (Dawson et al., 2009). Coastal storms are a combination of multiple disasters that can affect a coastline. Among these, coastal erosion can result in a significant economic loss by damaging buildings, roads, infrastructure, natural resources, and wildlife habitats. This erosion is caused by factors such as rising local sea levels, strong wave action, and floods, leading to the removal of rocks and soils from the coastline. The resulting damage to coastal infrastructure and land loss due to erosion in the USA costs over $500 million annually (*Coastal Erosion | U.S. Climate Resilience Toolkit*, n.d.; K. W. Liu et al., 2021). Therefore, it is essential to address the issue of coastal erosion, given the aging infrastructure and the increasing occurrence of severe weather.

In the past few decades, various methods have been developed to advance fundamental understanding and improve the coastal erosion resistance of sandy soil (Y.-J. Cheng et al., 2021; Jain & Kothyari, 2009a; Kou et al., 2020; Miftah et al., 2022). Geosynthetics are crucial in reinforcing earth structures and can be effectively used to protect slopes from erosion and improve stability (Ghiassian et al., 1997; Kim et al., 2019). Liu et al. (2019) used a water-based polyurethane soil stabilizer to reinforce the topsoil for sandy slope erosion control purposes (J. Liu et al., 2019). Utilizing vegetation is a common approach for slope protection, as it reduces water infiltration, retards erosion, and extracts moisture from the soil, ultimately contributing to slope stabilization (Bordoloi & Ng, 2020; Chirico et al., 2013; Kokutse et al., 2016). Yet, the extended duration of plant growth poses a challenge to the efficient application of the vegetation cover method (Bullock & King, 2011; Fattet et al., 2011). At the field scale, optimizing the mixture of geosynthetic materials and soil, as well as achieving a homogeneous state, is difficult (Steinberg, 1998). Various types of fibers have also been investigated as potential surface protection (Falamaki et al., 2023; Miller & Rifai, 2004; Tang et al., 2012). However, it should be highlighted that fiber distribution is critical to their effectiveness in soil strengthening (Chaduvula et al., 2017). When homogeneity is not preserved, cracks may initiate along the routes that offer the least resistance (Izzo & Miletić, 2022). Excessive utilization of chemical substances adversely affects the ecosystem (B. H. W. Cochrane et al., 2005). Hence, there is a pressing need for the development of a novel methodology to address the issue of erosion on shoreline slopes.

Enzyme-Induced Carbonate Precipitation (EICP) is a promising biocementation technique

that harnesses the power of enzymatic reactions to enhance soil quality and address various geotechnical challenges (A. Almajed et al., 2018; Dilrukshi et al., 2018; Hamdan, 2014; Javadi et al., 2021; Natarajan, 1995). EICP offers an eco-friendly approach for soil improvement and remediation by utilizing the hydrolysis of urea catalyzed by plant-derived urease enzymes. This technique involves the precipitation of calcium carbonate within the soil matrix, resulting in improved mechanical properties and environmental performance. Equations (i)–(v) summarize the main chemical reactions during biocementation (Saif et al., 2022). Equation (i) shows the hydrolysis of urea, which produces ammonia and carbamic acid, thus increasing pH. Carbamic acid is further hydrolyzed into ammonia plus carbonic acid. According to Equations (iii) and (iv), the reactions then generate ammonium and carbonate ions alongside hydroxide ions, further increasing the reaction medium's pH. Finally, equation (v) indicates that the reaction between carbonate ions and calcium ions leads to the precipitation of calcium carbonate once supersaturation is attained.

$$CO(NH_2)_2 + H_2O \longrightarrow NH_2COOH + NH_3 \quad \text{(i)}$$

$$NH_2COOH + H_2O \longrightarrow NH_3 + H_2CO_3 \quad \text{(ii)}$$

$$2NH_3 + 2H_2O \longrightarrow 2NH_4^+ + 2OH^- \quad \text{(iii)}$$

$$2OH^- + H_2CO_3 \longrightarrow CO_3^{-2} + 2H_2O \quad \text{(iv)}$$

$$Ca^{+2} + CO_3^{-2} \longrightarrow CaCO_3 \quad \text{(v)}$$

This study seeks to create a bio-mediated approach employing enzyme-induced calcite precipitation (EICP) to enhance the physical characteristics of coastal sand. Additionally, model-scale laboratory tests will be conducted to assess the effectiveness of this technique in mitigating coastal erosion.

## 2 Methodology

### 2.1 Beach Sand

In this study, the soil sample was collected from the subsurface along the coast of New Jersey (39°20'53.3"N 74°27'20.2"W) to design and assess the bio-mediated method for N.J. coastal embankment protection. Soil samples were put in the oven at 110°C for 24 hours to dry completely. Subsequently, the dry soil samples were subjected to sieving, wherein any particulate matter exceeding the retention threshold of a No. 4 sieve was removed. The laboratory analysis of these

soil samples was then conducted to obtain various physical properties, encompassing specific gravity, particle size distribution, bulk density, and permeability. The particle size distribution is shown in Figure 1.

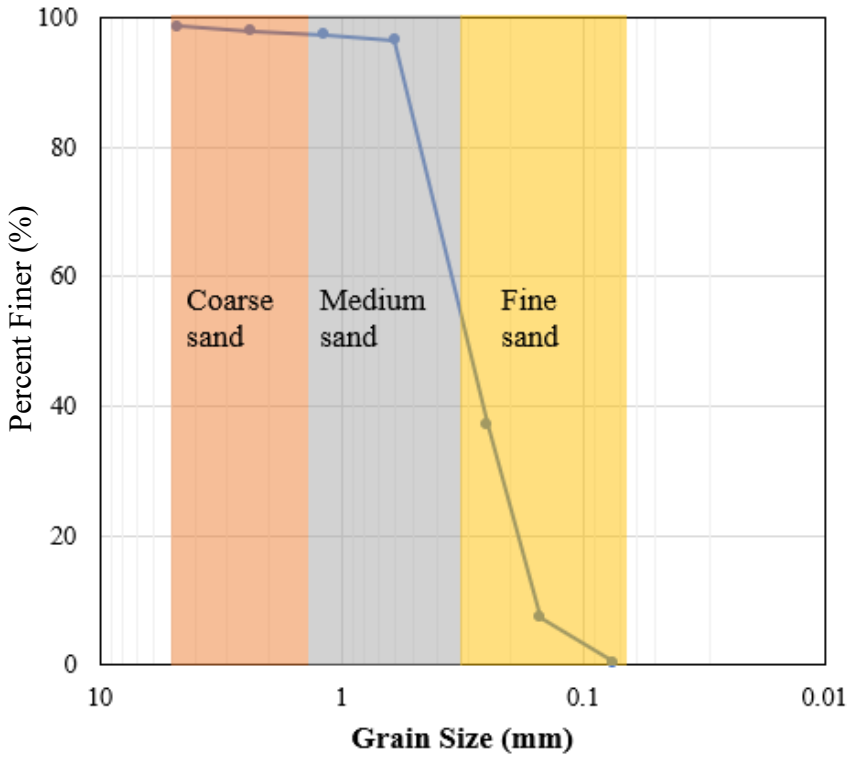


***Figure 1.*** *Particle size distribution of coastal sand sample*

According to the USCS, this soil can be identified as poorly graded sand (SP). Table 1 presents the physical properties of soil.

***Table 1.*** *Physical properties of experimental soil*

| **Physical properties** | **Values** |
|---|---|
| Specific gravity | 2.619 |
| Soil classification | SP |
| Maximum bulk density (kN /m$^3$) | 17.15 |
| Minimum bulk density (kN /m$^3$) | 15.58 |
| Hydraulic conductivity (cm/s) | 0.0103 |

## 2.2 EICP Solution

The enzyme-induced carbonate precipitation was prepared using cementation and an enzyme solution mixed at a 1:1 ratio. Deionized (DI) water, nonfat milk powder (4 g/L), and 0.675 M calcium chloride were used to create the cementation solutions (A. A. Almajed, 2017). To obtain the enzyme solution, soybean seeds were initially pulverized and filtered using a #100 sieve to extract the soybean powder. Before utilization, the soybean powder was stored in a refrigeration unit maintained at a temperature of 4°C. The powder was combined with deionized water at various concentrations and agitated using a magnetic stirrer to achieve a uniform suspension solution. Subsequently, the solution was transferred into centrifuge tubes and subjected to centrifugation at 3000 revolutions per minute (rpm) for 15 minutes.

## 2.3 Urease Activity

The urease activity was determined by the electrical conductivity method following procedures provided in previous studies (Pandey, 2018; Whiffin, 2004). The enzymatic activity was determined by converting the slope of the conductivity change over time using an appropriate conversion factor at $25^0$ C and pH 7 at standard conditions. To conduct this analysis, urea solutions of varying concentrations (150mM, 300mM, and 375mM) were prepared in separate beakers. The urease enzyme solution was added to achieve the desired urea concentration and a total volume containing 0.5gm/L of urease. After allowing sufficient time for complete urea hydrolysis, conductivity readings were recorded, including intermittent measurements to monitor changes over time. Electrical conductivity measurements were conducted on a solution contained within a glass vial. In this experiment, 5 ml of urease solution was added to a vial containing 15 ml of urea solution, resulting in an overall concentration of 1.5M for urea and 0.5 gm/L for urease (Pandey, 2018). Conductivity readings were recorded at intervals of 0, 1, 2, 3, 4, 5, 6, 7, and 8 minutes. These conductivity test results were graphed against time, and the slope obtained from the graph was converted to enzyme activity by multiplication with an appropriate conversion factor.

## 2.4 Test Tube Experiment

A series of precipitation studies were conducted using test tubes to assess the impact of initial chemical conditions on the enzyme-induced chemical precipitation (EICP) process and its reactivity. Several parameters influenced the precipitation, and its relationship with precipitation was examined by influencing variables such as pH, temperature, and enzyme concentrations. The

impact of pH on precipitation was examined by manipulating pH levels using varying quantities of 0.1M NaOH or 0.1 M HCl in the cementation solution. The cementation and enzyme solutions were made individually to carry out the test tube experiment. The solutions were mixed in a 1:1 ratio and allowed to undergo a precipitation process in a test tube at a predetermined temperature for 6 days. According to prior literature, the estimated duration for the completion of the reaction is 48 hours (Albenayyan et al., 2023). However, it is often observed that lower temperatures tend to decrease the rate of chemical reactions. Following the completion of the curing period, the resultant fluid was subjected to filtration. Calcium carbonate precipitation was measured in two ways. After the filtration, 5ml liquid was collected to measure the Ca ion concentration using an Atomic Absorption Spectrophotometer (AAS). After completion of the experiment, both pH and electrical conductivity were measured at room temperature.

## 2.5 Design of Experiments

A complete factorial design was utilized for the experimental design, incorporating three factors with three levels for each factor. Full factorial designs systematically investigate all potential combinations of factor levels to observe their effects on the outcomes (Colette et al., 2023; Kumar et al., 2015; Zhang et al., 2022). Each unique combination is known as a treatment combination (Buragohain & Mahanta, 2008). This approach will help understand how these factors and their interactions impact the experimental results. In our case, we focused on three independent factors: pH, temperature, and enzyme concentration. These factors were studied at three levels, as shown in Table 2.

***Table 2.*** *Factors and their levels for Design of Experiments (DOE)*

| **Factors** | **Levels** | **Values** |
|---|---|---|
| **pH** | 3 | 6, 7, 8 |
| **Enzyme Concentration (g/L)** | 3 | 60, 90, 120 |
| **Temperature ($^0$C)** | 3 | 10, 30, 50 |

The software suggested $3^3 = 27$ experimental runs to analyze the influence of each factor and their interactions. An example of a statistical test run is shown in Table 3. Here, run order is the order of experimental runs, and std order stands for the typical order of the experimental runs.

To analyze the results and optimize conditions for setting the control factors, Minitab 17 statistical software was used.

***Table 3.*** *Example of test run from Minitab software*

| **Test run** | | **Variables** | | |
|---|---|---|---|---|
| **Std Order** | **Run Order** | **Temperature ($^0$ C)** | **pH** | **Enzyme Conc. (g/L)** |
| 14 | 1 | 30 | 7 | 90 |
| 2 | 2 | 10 | 6 | 90 |
| 21 | 3 | 50 | 6 | 120 |
| 16 | 4 | 30 | 8 | 60 |
| 20 | 23 | 50 | 6 | 90 |
| 1 | 24 | 10 | 6 | 60 |
| 12 | 25 | 30 | 6 | 120 |
| 26 | 26 | 50 | 8 | 90 |
| 15 | 27 | 30 | 7 | 120 |

## 2.6 Permeability Test

To measure the hydraulic properties of the samples, the specimens were prepared in a permeability cell with an internal diameter of 84 mm and a height of 278 mm to measure the hydraulic conductivity changes based on the EICP treatment. The dry density of 1.47 g/cm$^3$ was achieved by layering sand in the cell and softly compacting it in 3 layers for specimens to be used for EICP treatment. After that, the specimen was saturated with a predetermined amount of EICP solution from the bottom up for the first cycle of treatment. After six days of curing, the next cycle begins. Figure 2 shows the test setup for hydraulic conductivity.

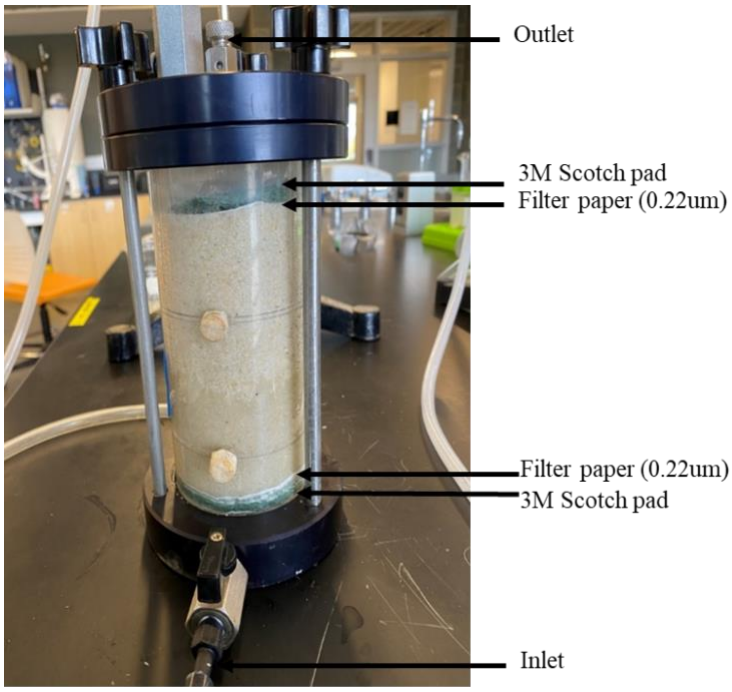


***Figure 2.*** *Test setup for hydraulic conductivity*

## 2.7 Direct Shear Test

In this study, a direct shear apparatus with a circular mold with an internal diameter of 63 mm was utilized. The beach sand was subjected to one cycle or two cycles of treatment. Untreated beach sand specimens were also tested as controls. All tests were conducted in triplicate and dry conditions in accordance with ASTM 3080. The inner side of the mold was covered with petrolatum and a thin plastic sheet in order to extract the resulting specimen smoothly without breaking the sand column. The sand was poured freely to achieve 1.9 g/cm$^3$ dry density. Each cycle of treatment was applied by percolating one pore volume of EICP cementation solution (i.e., 35 mL of EICP solution). Figure 3 shows the molded sample for the direct shear test. Each specimen was cured for six days per treatment cycle at room temperature.


(a) (b)

***Figure 3.*** *Direct shear stress test sample (a) treated soil column; (b) after shear failure*

## 2.8 Soil Erosion Model Tank

Model-scale laboratory tests were often conducted by researchers to study the erosion mechanism of sandy slopes (Kou et al., 2020; K. W. Liu et al., 2021). In this study, similar principles were followed to perform wave erosion tests. The testing system consists of a rectangular cuboid container that is 30-in in length, 12-in in width, and 18-in in height, a high-resolution camera, and a propeller-based wave-maker. The wave-maker was installed at one side of the container to generate regular sinusoidal waves using a periodic propeller pump. This experimental investigation was not aimed at completely replicating the sandy slope erosion process in the laboratory. The main focus was to assess the efficacy of EICP treatment in a sandy slope exposed to wave conditions while considering the scaling laws associated with beach sandy slope erosion processes. The sand was maintained with 8% moisture content as the original condition and compacted in the tank at 1.44 gm/cm$^3$. The slope will follow a planar cross-shore sandy slope profile with slope angles of 30°. The spraying treatment method (Q. Cheng et al., 2021; Roksana et al., 2023) was employed in this investigation to stabilize the surface of the sandy slope. Firstly, the cementation and enzyme solution were mixed in a 1:1 ratio and sprayed uniformly on the surface of the sandy slope at a rate of 50ml/min using a spray bottle. A total of 1 L of cementation and enzyme was used to treat the slope surface. A control sample without any treatment was also prepared to compare the coastal erosion outcome before and after the EICP treatment. A high-resolution camera continuously monitored the erosion process indicated by the change in the cross-shore profile. Further image analysis of erosion volume and degree of slope reduction under wave

action was done based on the captured images of the cross-shore profile. Figure 4 represents the schematic diagram of the model tank.

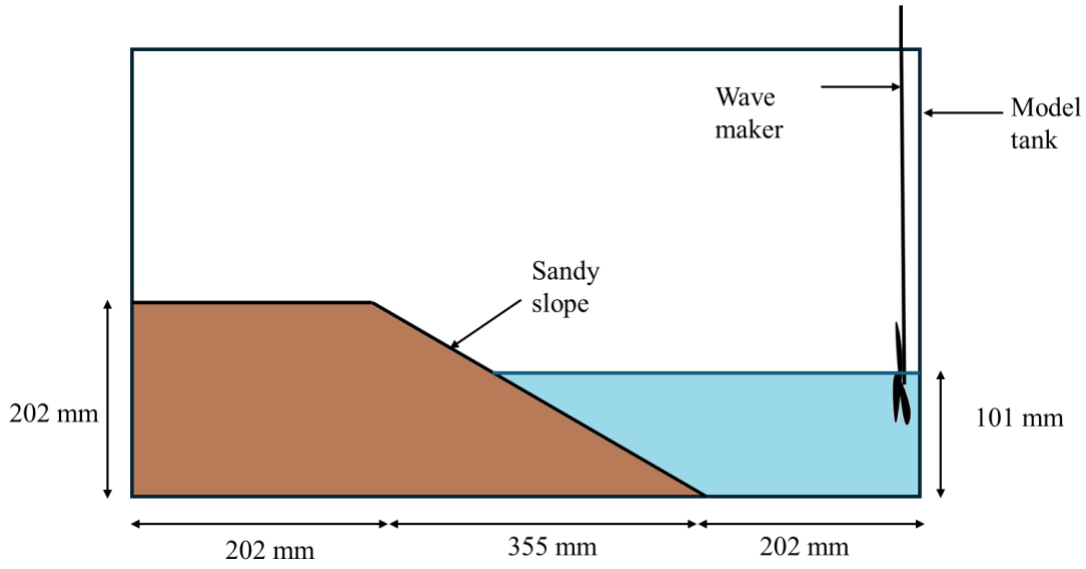


***Figure 4.*** *Schematic diagram of model tank*

## 3 Results and Discussion

### 3.1 Urease Activity of Soybean

The assessment of soybean crude urease solutions generated from soybean powder was conducted. Initially, standard curves were established for soybean crude urease, as illustrated in Figure 5.

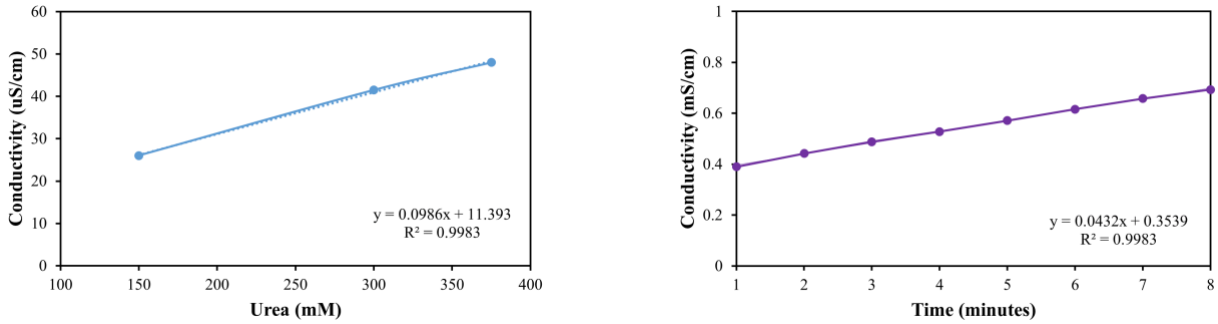


(a) (b)

***Figure 5.*** *(a) Standard curve for soybean crude extract urease; (b) Electrical conductivity vs. time for 60 g/L concentration*

The electrical conductivity (EC) changes in Figure 5(a) exhibited a nearly linear trend with an $R^2$ value close to 1 and a slope of 0.0986. From the graph, the relationship between urea hydrolysis and conductivity is given in equation (vi)

$$\text{Urea hydrolyzed (mM)} = \text{Conductivity (µS/cm)} * 10.14 \qquad \text{(vi)}$$

The value of the conversion factor is consistent with some previous studies. For example, Whiffin (2004) got a factor of 11.11, while Pandey (2018) got a factor of 10.24 (Pandey, 2018; Whiffin, 2004).

$$\text{Urease activity} = \text{slope} * 1000 * 10.14 \qquad \text{(vii)}$$

The results for 60g/L soybean crude urease enzyme concentrations are 438 µM urea/min, as illustrated in Figure 5 (b).

### 3.2 $CaCO_3$ Optimization

The study aims to determine the ideal pH, temperature, and enzyme concentration that will result in the highest level of carbonate precipitation. The tube test results were examined based on the smallest amount of Ca ion in the solution to determine the optimal EICP solution.

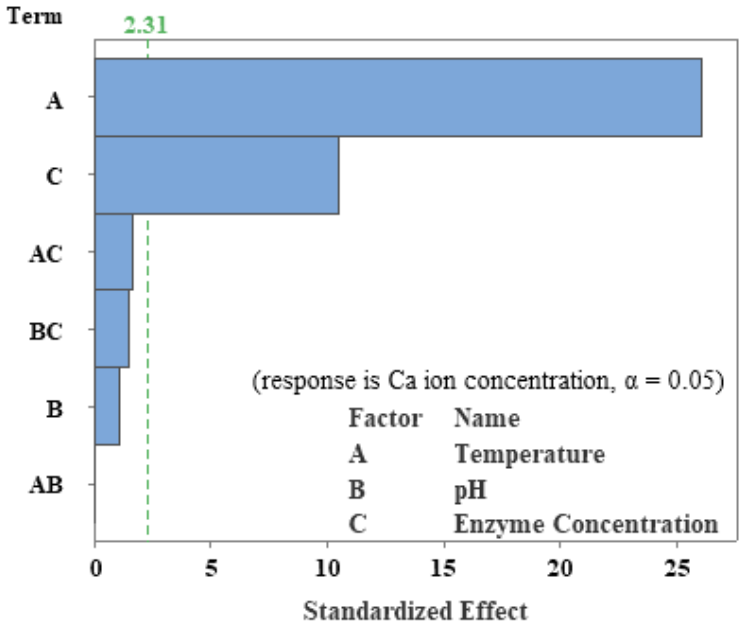


***Figure 6.*** *Pareto chart of the standardized effect*

A total of 27 test samples were run by varying temperature, pH, and enzyme concentration. After 6 days of curing, a 5 ml solution is collected from each tube, and the calcium ion concentration is measured with a 230 ATS Atomic Absorption Spectrophotometer.

Figure 6 illustrates the standardized effects of temperature, pH, and enzyme concentration in response to the Ca concentration at alpha=0.05. This chart explains the interaction of various combinations of the parameters in the production of Ca. Based on the reference line (green dotted line), only temperature and enzyme concentration significantly affect Ca production in the range tested. Neither of the combinations of the two parameters was found to impact the production of Ca significantly. The chart also reveals that temperature has a higher impact on Ca production, followed by enzyme concentration. Based on the chart, it can be inferred that temperature and enzyme concentration significantly impact Ca production.

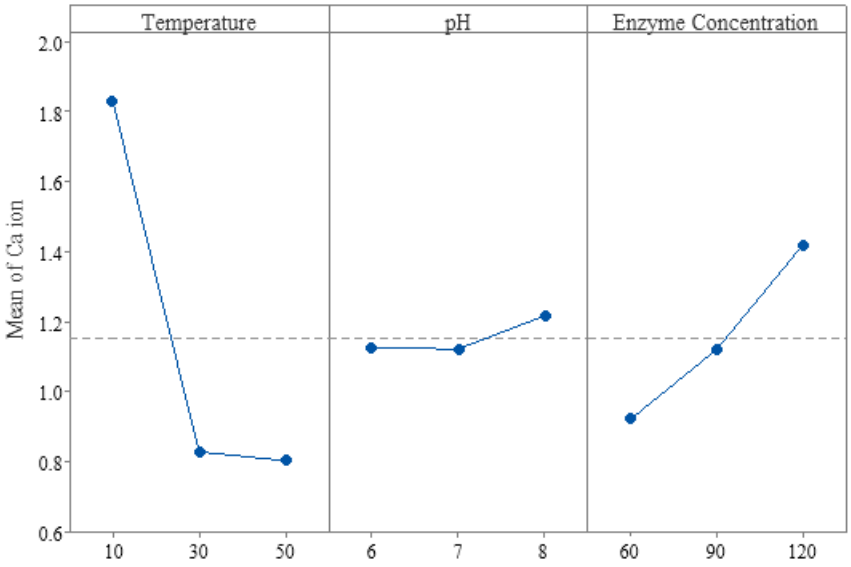


***Figure 7.*** *Main effect plot for Ca ion concentration*

Figure 7 illustrates the main effects of the parameters (temperature, pH, enzyme concentration) for Ca ion concentration. As seen in the figure, an increase in temperature decreases the Ca production until $30^0$C, and it increases again. Hence, a temperature of $30^0$C is optimum for optimal Ca value. An increase in enzyme concentration increases Ca production. Hence, an optimal concentration of 60 g/L is obtained for the Ca production. It is worth mentioning that pH has little impact on Ca production, with a pH of 7 having the optimal Ca concentration. Based on

the results, the optimal solution could be obtained at a pH of 6, with $30^0$C and an enzyme concentration of 60 g/L. The lowest Ca ion concentration under this condition becomes 0.41 ppm.

### 3.3 Permeability Test Results

We investigated the effect of Enzyme-Induced Carbonate Precipitation (EICP) on the permeability of coastal soil. Since calcite precipitation is known to reduce the soil's permeability, constant head permeability tests were conducted to determine the extent of the reduction. The result showed that the coefficient of permeability decreased effectively with the increasing number of EICP treatment cycles. Since biocementation occurs in pores within soil particles, reducing the pore throats and subsequently preventing water flow (Whiffin et al., 2007). Figure 8 represents the control sample permeability constant along with 1, 2, and 3 cycles of treatment. The control sample's permeability was 0.01 cm/s, whereas it was reduced to 0.005, 0.002, and 0.001 cm/s with treatment cycles one, two, and three, respectively.

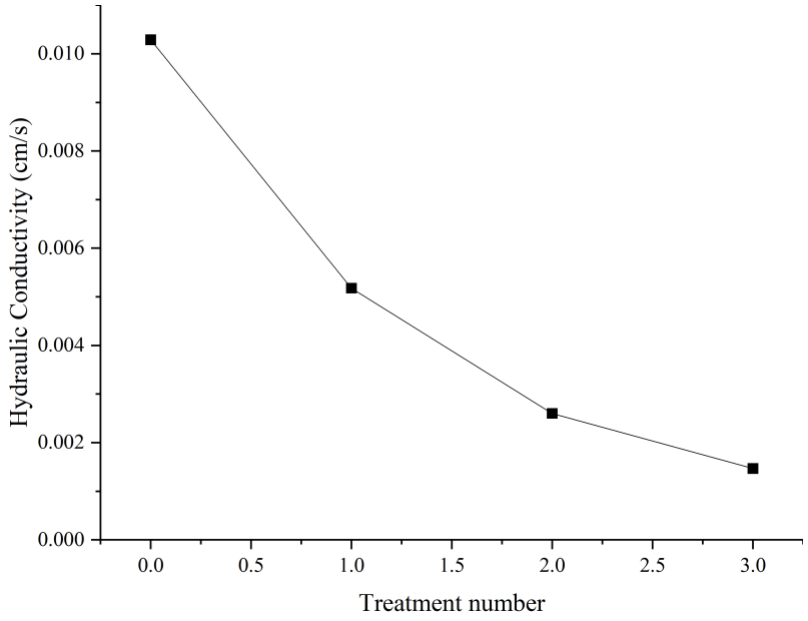


***Figure 8.*** *Effect of EICP treatment cycles on the permeability constant of coastal sand*

### 3.4 Direct Shear Test Result

Figure 9 shows the relationship between normal stress and maximum shear stress under different treatment conditions. Maximum shear stress increases with the increasing treatment cycle for a given normal stress. For the natural sand samples, the cohesion is 0 kPa, and the internal friction angle is equal to 34.21 degrees. The cohesion for bio-cemented sand with one cycle

increases to 17 kPa, and the internal friction angle increases to 32.21 degrees. After two cycle treatments, cohesion increases to 30 kPa, and friction angle decreases to 31.78 degrees.

The increase in shear strength can be attributed to the increase in cohesion. However, the angle of friction remained fairly stable throughout the treatment cycle. An inverse relationship between soil cohesion and soil particle detachment has been confirmed. At lower confining pressures, a significant increase in cohesion dominates the reduction in internal frictional angle, directly affecting erosion (Jain & Kothyari, 2009b, 2009a; Torri et al., 1987). Induced cohesion at lower confining pressures helps to mitigate coastal erosion, which is predominantly a surface phenomenon. Even at low confining pressures, the development of cohesion will decrease the erosion rate as well as the magnitude (Miftah et al., 2022). Hence, biocementation has been proven to enhance the qualities of sandy soil in terms of cohesiveness and internal friction angle.

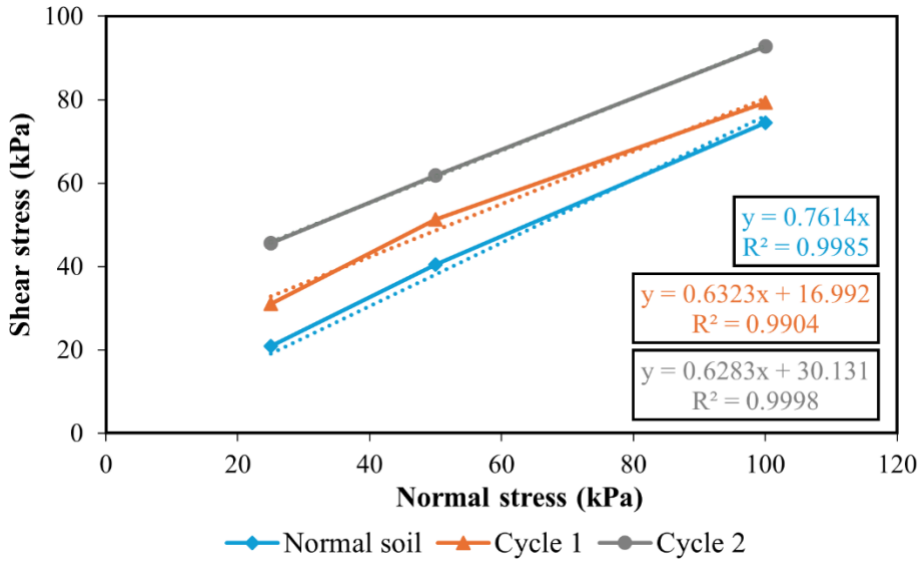


***Figure 9.*** *Relationship between normal stress and shear stress of treated and untreated sand*

### 3.5 Erosion Characteristics of Sandy Slope Under wave Action

This laboratory-scale soil erosion test was conducted on untreated and EICP-treated soil. As illustrated in Figure 10, the initial slope was straight at time=0, and upon the application of waves, the slope gradually began to break. From the beginning, the slope begins to collapse, manifesting as a break at the point impacted by the water's surface. Given that the wave was generated at the water's surface, the maximum force was exerted on the slope near this region. By t=5 minutes, the

bottom of the slope exhibited increased erosion compared to its initial state, and this trend persisted. At t=9 minutes, the lower part of the slope had undergone substantial reduction. Examining the rate of slope change under wave over time provides valuable insights into how untreated normal soil reacts to wave action in shoreline areas.

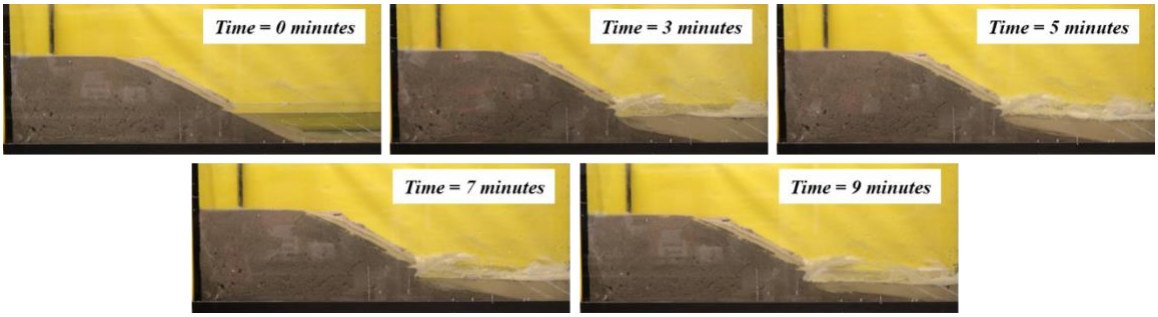


***Figure 10.*** *Cross-section profile of untreated sandy slope as a function of time*

In contrast, EICP-treated soil underwent the same wave experiment as the untreated soil to assess its efficacy in slope resistance, as depicted in Figure 11. At time=0, the slope was initially straight. Unlike untreated soil, the EICP-treated slope took longer to exhibit any signs of breaking, and visible changes were not immediately apparent. No visible breaks were observed at the point of impact with the water's surface, and this structural integrity persisted throughout the observation period.

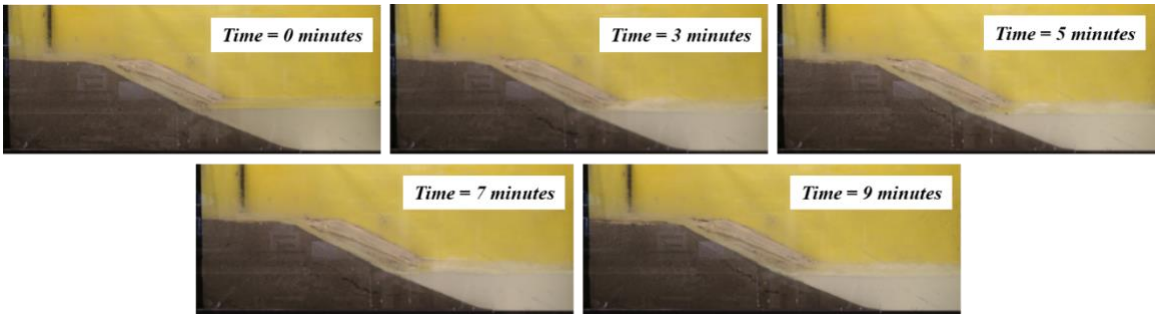


***Figure 11.*** *Cross-section profile of EICP treated sandy slope as a function of time*

While these changes may not be readily apparent to the naked eye, computer vision analysis captured subtle variations in volume above the still water level. Examining the rate of slope change over time provides valuable information on how EICP-treated soil reacts to wave impact in

shoreline areas. Both figures unequivocally indicate that the performance of EICP-treated soil surpasses that of untreated soil in maintaining slope stability.

The erosion process of the sandy slope with and without the implementation of EICP treatment has been systematically investigated, and some observations are depicted in Figure 10 and Figure 11. It was found that for the slope without EICP treatment, as the wave struck the slope surface, a large amount of sand was eroded away. On the contrary, the slope surface experienced minor erosion during EICP treatment. The cementation effect can lead to an increase in shear strength, as well as a higher erosion resistance. Figure 10 illustrates the impact of wave action on an untreated sandy slope, revealing significant sand erosion upon wave contact. In contrast, the slope subject to EICP treatment exhibited minimal erosion due to the cementation effect, resulting in increased shear strength and heightened resistance to erosion. To quantitatively evaluate the erosion process, the degree of erosion (De) was computed by measuring the decrease in slope angle.

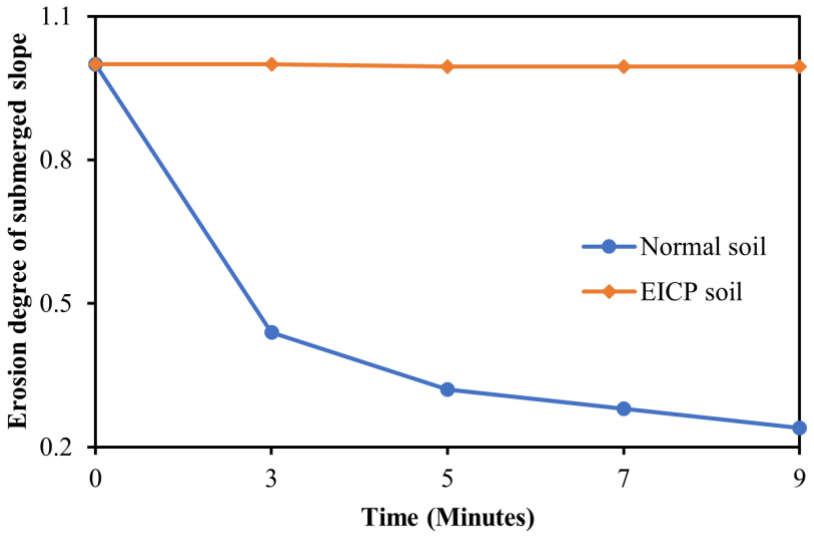


***Figure 12.*** *Change of erosion degree of submerged slope as a function of time*

Figure 11 highlights that the eroded slope surface displays a bilinear profile characterized by a slope inclination influenced by wave action and a submerged slope angle. These two angles distinctly differ due to varying erosion impacts. The erosion degree (De) was determined by the ratio of the eroded degree and the initial degree. According to this definition, the erosion degrees for the untreated slope were calculated as 0.44, 0.32, 0.28, and 0.24 at 3, 5, 7, and 9 minutes, respectively. Conversely, for the EICP-treated sand, the erosion degree remained relatively

constant over time, nearly reaching 1 after an extended period. The change of erosion degree of submerged slope is shown in Figure 12.

Figure 13 depicts the temporal evolution of erosion volume above the still water level in response to wave action. The erosion volume above the still water level was determined by computing the difference between the initial bed profile above the water level and the measured profile after a specified duration. Bio-mediated treatments demonstrated a noteworthy reduction in erosion volume. Specifically, the untreated soil sample resulted in erosion volumes of 7%, 8%, 10%, and 11% at 3, 5, 7, and 9 minutes, respectively. Compared to the EICP treatment, the erosion rate exhibited decreases of 1%, 1%, 2%, and 6% at 3, 5, 7, and 9 minutes, respectively.

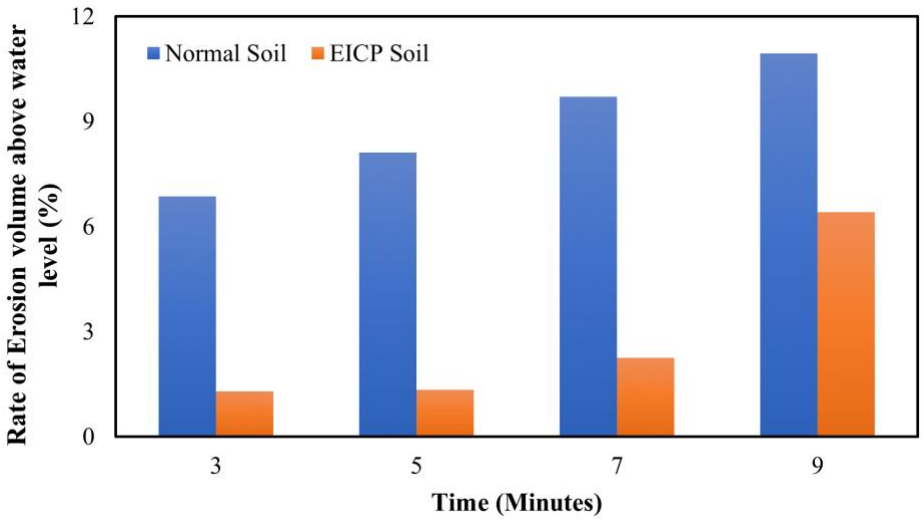


***Figure 13.*** *Rate of erosion volume above water level as a function of time*

### 3.6 Microscopic characteristics

The scanning electron microscope (SEM) was used to observe the changes in the microscale structure of untreated and treated beach sand and to identify the morphology of $CaCO_3$ precipitates. Figure 14 (a) and (b) show the SEM images of the treated and untreated sand. The spherical crystals in the treated specimens demonstrate the presence of calcite. The precipitates were observed at inter-particle contacts and on the surface of the particles. This finding may also be important for explaining the mechanism of improving the cohesion and reducing the permeability of treated sand, where the cohesion was increased, and permeability was decreased with the increase of $CaCO_3$ content.

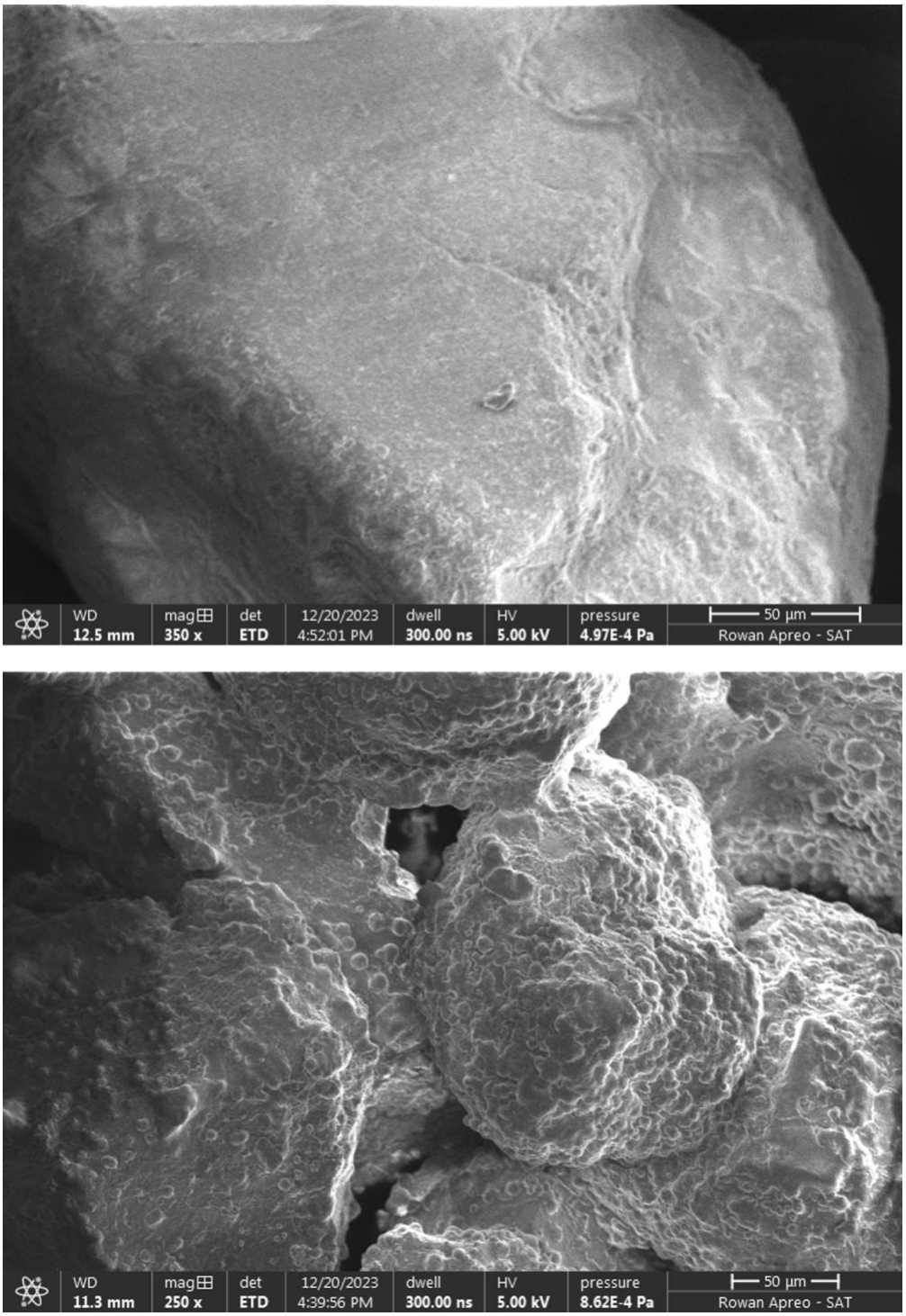


***Figure 14.*** *Scanning Electronic Microscope (SEM) image (a) untreated sand; (b) treated sand coated with calcium carbonate crystal*

Figure 15 (a) illustrates the surface characteristics of the topsoil subsequent to undergoing EICP treatment. This treatment results in the formation of a distinct layer atop the soil surface.

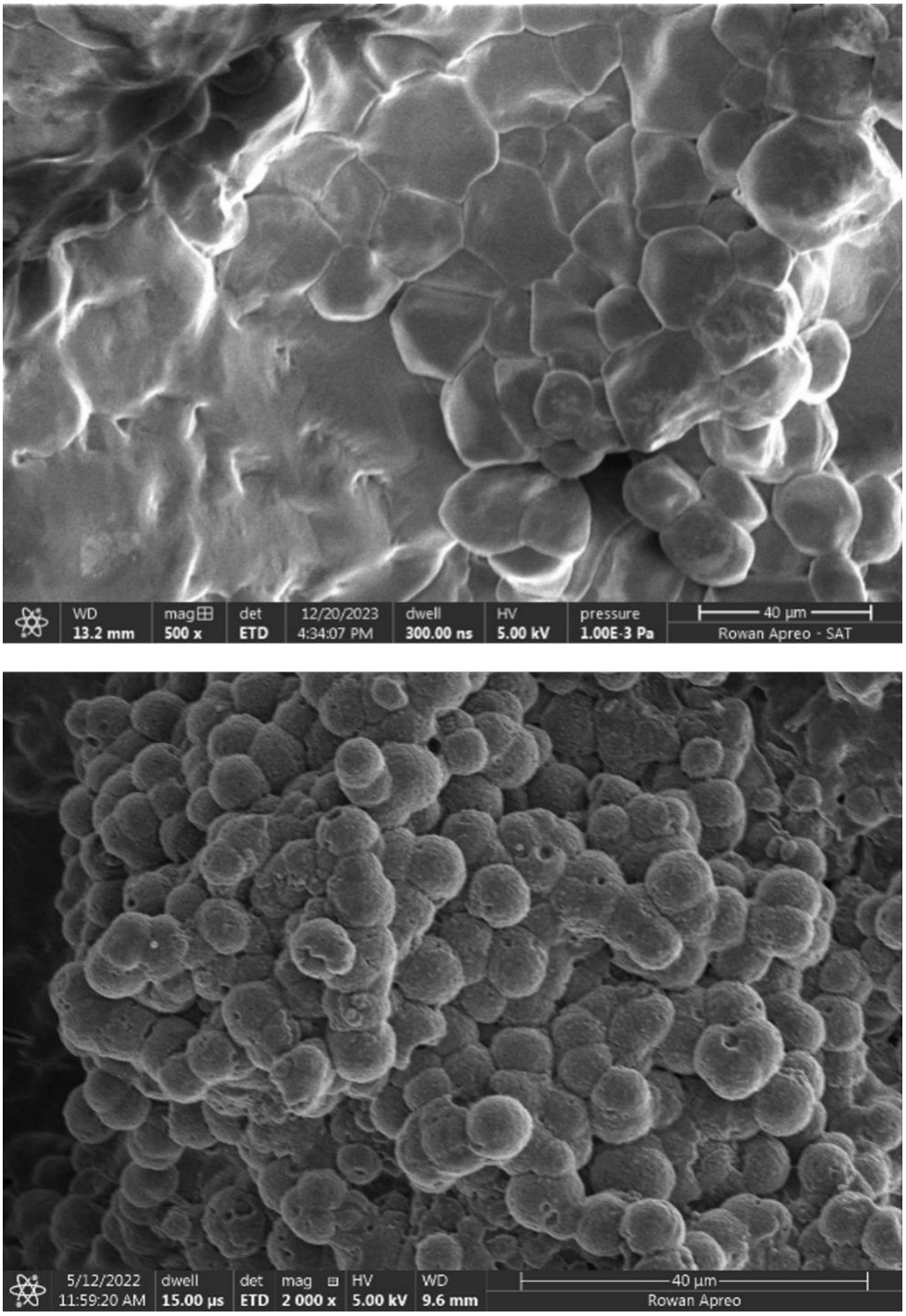


***Figure 15.*** *Scanning Electronic Microscope (SEM) image (a) hard layer of crystals in soil surface; (b) cluster of calcium carbonate (vaterite)*

This top layer reduced the rate of water absorption compared to soil treated solely with water, as observed during the wetting process (Roksana et al., 2023). It has also been found that the existence

of a top hard layer impedes the infiltration of water into the soil, leading to an extended period of time required for water absorption and evaporation by the soil (Y.-J. Cheng et al., 2021). Based on the SEM image in Figure 15 (b), it can be observed that the precipitates in the soil consist primarily of spherical calcium carbonate crystal vaterite, with some amorphous aragonites present as well. These minerals are known to be less stable than calcite crystals. When precipitation occurs rapidly at high levels of supersaturation, these forms, which are the least thermodynamically stable, appear and rapidly convert to a more stable anhydrous phase. This may happen due to the presence of impurities in the raw materials.

## 4 Conclusions

The study focused on the innovative enzymatic-induced carbonate precipitation (EICP) method as a bio-mediated solution for mitigating coastal erosion problems. The research demonstrated a substantial reduction of sandy slope erosion under wave conditions through comprehensive assessments of soil properties and small-scale laboratory model tests on EICP-treated and untreated sandy slopes. Experimental results showed that EICP-treated coastal sand improved the shear strength and permeability characteristics. The permeability decreases as the number of EICP treatment cycles increases due to the filling of soil pores with calcium carbonate precipitation. A significant increase in shear strength was also observed due to increasing $CaCO_3$ content at a given confining pressure. The increase in strength was majorly attributed to an increase in cohesion. Meanwhile, a decrease in the internal frictional angle was observed in the treated specimens. Small-scale laboratory erosion tests prove that EICP effectively mitigates the erosion of sandy slopes. The SEM results of the treated beach sand showed the presence of vaterite as the predominant crystal phase of the enzyme-induced carbonate precipitates in all treated specimens. The outcomes of this study showed strong evidence of the applicability of using enzyme-induced carbonate precipitation (EICP) treatment for beach sand strengthening against soil erosion.

## 5 Acknowledgement

This study is funded by Camden Health Research Initiative of Rowan University. This publication was supported by a subaward from Rutgers University, Center for Advanced Infrastructure & Transportation, under Grant no. 69A3551847102 from the U.S. Department of

Transportation, Office of the Assistant Secretary for Research and Technology (OST-R). Any opinions, findings, and conclusions or recommendations expressed in this publication are those of the author(s) and do not necessarily reflect the views of Rutgers, the State University or those of the U.S. Department of Transportation, Office of the Assistant Secretary for Research and Technology (OST-R).

## References


Albenayyan, N., Murtaza, M., Alarifi, S. A., Kamal, M. S., Humam, A., AlAhmari, M. M., Khalil, A., & Mahmoud, M. (2023). Optimization of calcium carbonate precipitation during alpha-amylase enzyme-induced calcite precipitation (EICP). *Frontiers in Bioengineering and Biotechnology*, *11*, 1118993. https://doi.org/10.3389/FBIOE.2023.1118993/BIBTEX

Almajed, A. A. (2017). *Enzyme Induced Carbonate Precipitation (EICP) for Soil Improvement*. Arizona State University.

Almajed, A., Khodadadi Tirkolaei, H., & Kavazanjian, E. (2018). Baseline Investigation on Enzyme-Induced Calcium Carbonate Precipitation. *Journal of Geotechnical and Geoenvironmental Engineering*, *144*(11), 04018081. https://doi.org/10.1061/(ASCE)GT.1943-5606.0001973

B. H. W. Cochrane, J. M. Reichert, F. L. F. Eltz, & L. D. Norton. (2005). CONTROLLING SOIL EROSION AND RUNOFF WITH POLYACRYLAMIDE AND PHOSPHOGYPSUM ON SUBTROPICAL SOIL. *Transactions of the ASAE*, *48*(1), 149–154. https://doi.org/10.13031/2013.17958

Bordoloi, S., & Ng, C. W. W. (2020). The effects of vegetation traits and their stability functions in bio-engineered slopes: A perspective review. *Engineering Geology*, *275*, 105742. https://doi.org/10.1016/j.enggeo.2020.105742

Bullock, A., & King, B. (2011). Evaluating China's Slope Land Conversion Program as sustainable management in Tianquan and Wuqi Counties. *Journal of Environmental Management*, *92*(8), 1916–1922. https://doi.org/10.1016/j.jenvman.2011.03.002

Buragohain, M., & Mahanta, C. (2008). A novel approach for ANFIS modelling based on full factorial design. *Applied Soft Computing*, *8*(1), 609–625. https://doi.org/10.1016/J.ASOC.2007.03.010

Chaduvula, U., Viswanadham, B. V. S., & Kodikara, J. (2017). A study on desiccation cracking behavior of polyester fiber-reinforced expansive clay. *Applied Clay Science*, *142*, 163–172. https://doi.org/10.1016/j.clay.2017.02.008

Cheng, Q., Tang, C.-S., Xu, D., Zeng, H., & Shi, B. (2021). Water infiltration in a cracked soil considering effect of drying-wetting cycles. *Journal of Hydrology*, *593*, 125640. https://doi.org/10.1016/j.jhydrol.2020.125640

Cheng, Y.-J., Tang, C.-S., Pan, X.-H., Liu, B., Xie, Y.-H., Cheng, Q., & Shi, B. (2021). Application of microbial induced carbonate precipitation for loess surface erosion control. *Engineering Geology*, *294*, 106387. https://doi.org/10.1016/j.enggeo.2021.106387

Chirico, G. B., Borga, M., Tarolli, P., Rigon, R., & Preti, F. (2013). Role of Vegetation on Slope Stability under Transient Unsaturated Conditions. *Procedia Environmental Sciences*, *19*, 932–941. https://doi.org/10.1016/j.proenv.2013.06.103

*Coastal Erosion | U.S. Climate Resilience Toolkit*. (n.d.). Retrieved January 12, 2024, from https://toolkit.climate.gov/topics/coastal-flood-risk/coastal-erosion

Colette, D. A., Martial, A. K. D., Joseph, A. Y., Benjamin, Y. K., & Patrick, D. A. (2023). Optimization of the compressive strength of used tire/cement phase composite concretes using a full factorial design. *Construction and Building Materials*, *404*. https://doi.org/10.1016/j.conbuildmat.2023.133252

Dilrukshi, R. A. N., Nakashima, K., & Kawasaki, S. (2018). Soil Improvement using Plant-derived Urease-induced Calcium Carbonate Precipitation. *Soils and Foundations*, *58*(4), 894–910. https://doi.org/10.1016/j.sandf.2018.04.003

Falamaki, A., Salimi, M., Vakili, A. H., Homaee, M., Aryanpour, M., Sabokbari, M., Dehghani, R., Masihzadeh, K., & Karimi, A. H. (2023). Experimental investigation of the effect of landfill leachate on the mechanical and cracking behavior of polypropylene fiber-reinforced compacted clay liner. *Environmental Science and Pollution Research*. https://doi.org/10.1007/s11356-023-27512-1

Fattet, M., Fu, Y., Ghestem, M., Ma, W., Foulonneau, M., Nespoulous, J., Le Bissonnais, Y., & Stokes, A. (2011). Effects of vegetation type on soil resistance to erosion: Relationship between aggregate stability and shear strength. *CATENA*, *87*(1), 60–69. https://doi.org/10.1016/j.catena.2011.05.006

Ghiassian, H., Gray, D. H., & Hryciw, R. D. (1997). Stabilization of Coastal Slopes by Anchored Geosynthetic Systems. *Journal of Geotechnical and Geoenvironmental Engineering*, *123*(8), 736–743. https://doi.org/10.1061/(ASCE)1090-0241(1997)123:8(736)

Hamdan, N. (2014). *Applications of Enzyme Induced Carbonate Precipitation (EICP) for Soil Improvement*. Arizona State University.

Izzo, M. Z., & Miletić, M. (2022). Desiccation Cracking Behavior of Sustainable and Environmentally Friendly Reinforced Cohesive Soils. *Polymers*, *14*(7), 1318. https://doi.org/10.3390/polym14071318

Jain, R. K., & Kothyari, U. C. (2009a). Cohesion influences on erosion and bed load transport. *Water Resources Research*, *45*(6). https://doi.org/10.1029/2008WR007044

Jain, R. K., & Kothyari, U. C. (2009b). Cohesion influences on erosion and bed load transport. *Water Resources Research*, *45*(6). https://doi.org/10.1029/2008WR007044

Javadi, N., Khodadadi Tirkolaei, H., Hamdan, N., & Kavazanjian, E. (2021). Longevity of Raw and Lyophilized Crude Urease Extracts. *Sustainable Chemistry*, *2*(2), 325–334. https://doi.org/10.3390/suschem2020018

Kim, Y.-J., Kotwal, A. R., Cho, B.-Y., Wilde, J., & You, B. H. (2019). Geosynthetic Reinforced Steep Slopes: Current Technology in the United States. *Applied Sciences*, *9*(10), 2008. https://doi.org/10.3390/app9102008

Kokutse, N. K., Temgoua, A. G. T., & Kavazović, Z. (2016). Slope stability and vegetation: Conceptual and numerical investigation of mechanical effects. *Ecological Engineering*, *86*, 146–153. https://doi.org/10.1016/j.ecoleng.2015.11.005

Kou, H., Wu, C., Ni, P., & Jang, B.-A. (2020). Assessment of erosion resistance of biocemented sandy slope subjected to wave actions. *Applied Ocean Research*, *105*, 102401. https://doi.org/10.1016/j.apor.2020.102401

Kumar, L., Sreenivasa Reddy, M., Managuli, R. S., & Pai K., G. (2015). Full factorial design for optimization, development and validation of HPLC method to determine valsartan in nanoparticles. *Saudi Pharmaceutical Journal*, *23*(5), 549–555. https://doi.org/10.1016/J.JSPS.2015.02.001

Liu, J., Chen, Z., Kanungo, D. P., Song, Z., Bai, Y., Wang, Y., Li, D., & Qian, W. (2019). Topsoil reinforcement of sandy slope for preventing erosion using water-based polyurethane soil stabilizer. *Engineering Geology*, *252*, 125–135. https://doi.org/10.1016/J.ENGGEO.2019.03.003

Liu, K. W., Jiang, N. J., Qin, J. De, Wang, Y. J., Tang, C. S., & Han, X. Le. (2021). An experimental study of mitigating coastal sand dune erosion by microbial- and enzymatic-induced carbonate precipitation. *Acta Geotechnica*, *16*(2), 467–480. https://doi.org/10.1007/s11440-020-01046-z

Miftah, A., Khodadadi Tirkolaei, H., Bilsel, H., & El Naggar, H. (2022). Erodibility improvement and scour mitigation of beach sand by enzymatic induced carbonate precipitation.

*Geomechanics for Energy and the Environment*, *32*, 100354. https://doi.org/10.1016/j.gete.2022.100354

Miller, C. J., & Rifai, S. (2004). Fiber Reinforcement for Waste Containment Soil Liners. *Journal of Environmental Engineering*, *130*(8), 891–895. https://doi.org/10.1061/(ASCE)0733-9372(2004)130:8(891)

Natarajan, K. R. (1995). Kinetic Study of the Enzyme Urease from Dolichos biflorus. *Journal of Chemical Education*, *72*(6), 556. https://doi.org/10.1021/ed072p556

Pandey, G. (2018). *Feasibility Study of Water Based / Polymer Modified EICP for Soil Improvement Involving Recycled Glass Aggregate*.

Roksana, K., Hewage, S. A., Lomboy, M. M., Tang, C., Xue, W., & Zhu, C. (2023). Desiccation cracking remediation through enzyme induced calcite precipitation in fine-grained soils under wetting drying cycles. *Biogeotechnics*, 100049. https://doi.org/10.1016/J.BGTECH.2023.100049

Saif, A., Cuccurullo, A., Gallipoli, D., Perlot, C., & Bruno, A. W. (2022). Advances in Enzyme Induced Carbonate Precipitation and Application to Soil Improvement: A Review. *Materials*, *15*(3), 950. https://doi.org/10.3390/ma15030950

Steinberg, M. (1998). *Geomembranes and the Control of Expansive Soils in Construction*. McGraw-Hil.

Tang, C.-S., Shi, B., Cui, Y.-J., Liu, C., & Gu, K. (2012). Desiccation cracking behavior of polypropylene fiber–reinforced clayey soil. *Canadian Geotechnical Journal*, *49*(9), 1088–1101. https://doi.org/10.1139/t2012-067

Torri, D., Sfalanga, M., & Del Sette, M. (1987). Splash detachment: Runoff depth and soil cohesion. *CATENA*, *14*(1–3), 149–155. https://doi.org/10.1016/S0341-8162(87)80013-9

Whiffin, V. S. (2004). *Microbial CaCO3 precipitation for the production of biocement*. https://researchportal.murdoch.edu.au/esploro/outputs/doctoral/Microbial-CaCO3-precipitation-for-the-production/991005540291407891

Whiffin, V. S., van Paassen, L. A., & Harkes, M. P. (2007). Microbial Carbonate Precipitation as a Soil Improvement Technique. *Geomicrobiology Journal*, *24*(5), 417–423. https://doi.org/10.1080/01490450701436505

Zhang, S., He, F., Fang, X., Zhao, X., Liu, Y., Yu, G., Zhou, Y., Feng, Y., & Li, J. (2022). Enhancing soil aggregation and acetamiprid adsorption by ecofriendly polysaccharides hydrogel based on Ca2+- amphiphilic sodium alginate. *Journal of Environmental Sciences*, *113*, 55–63. https://doi.org/10.1016/J.JES.2021.05.042